Supporting Information

Donor-Acceptor Hydrogen-Bonded Organic Framework with Turn-on Fluorescence Response of Phenethylamine (Drug Analogue) via Single-Crystal to Single-Crystal Transformation

Yanhong Liu, Wenyan Dan, and Bing Yan*

School of Chemical Science and Engineering, Tongji University, 1239 Siping Road, Shanghai 200092, China

* Corresponding author: Bing Yan, Email: byan@tongji.edu.cn

Experimental Section

Materials and instruments:

Tris(4-(pyridin-4-yl)phenyl)amine (TPPA, 98%) was from Yanshen Technology Co., Ltd, China. All other reagents and solvents were commercially available and used as received without further purification. The crystalline phases of the samples were determined by Powder X-ray diffraction patterns (PXRD) on a Bruker D8 diffractometer with Cu Kα radiation (40 kV, 40 mA) over the range of 5 ~ 50° at a scan rate of $0.1°·S^{-1}$. Simulation of the PXRD spectra was carried out by the single-crystal data and diffraction-crystal module of the Mercury programThermogravimetric analyses (TGA) were conducted on a PerkinElmer thermogravimetric analyzer from 30 to 800 °C at a rate of $10 °C·min^{-1}$ in flowing N_2. Fourier transform infrared (FT-IR) spectra were recorded using a Nicolet IS10 infrared spectrophotometer. The fluorescence spectra were examined on an Edinburgh FLS920 fluorescence spectrometer at room temperature. ^1H nuclear magnetic resonance (^1H NMR) spectra of the dissolved sample (diluted d-DMSO) were recorded on a Bruker Avance III 400. The corresponding Commission Internationale de l'Eclairage (CIE) color coordinates were calculated based on the international CIE standards.

Single-crystal X-ray Crystallography

The crystal structure of the as-prepared single crystal was analyzed using a Bruker SMART APEX II CCD area detector X-ray diffractometer, applying Mo Kα radiation (λ = 0. 71073 Å) at 50 kV and 30 mA. The structures were solved by direct methods and refined by full-matrix least-squares methods on all F^2 data (Olex2). Non-hydrogen atoms were refined anisotropically. The positions of hydrogen atoms were calculated and refined isotropically. Crystal parameters and details of refinements are given in Table S1 and S2.

Computational methods of DFT

Density functional theory (DFT) calculations were carried out by using the Gaussian 09 package.[1] Molecular geometries were fully optimized at B3LYP/6-31G(d, p) level with the dispersion corrections with Grimme's D3 method.[2] All optimized structures were confirmed no imaginary frequency. The binding energy was calculated as

$$E(b) = E(AB) - E(A) - E(B)$$

Where E(AB) was the energy of complex, E(A) and E(B) represented the energies of isolated fragment.

Preparation of TPPA-TMA

Tris(4-(pyridin-4-yl)phenyl)amine (TPPA, 0.048 g, 0.1 mmol) and 1,3,5-benzenetricarboxylic acid (H₃TMA, 0.053 g, 0.25 mmoL) were mixed into a 20 mL methanol solution to form a mixture, which was treated with ultrasound for 5 min. The mixture was heated for about 3 h at 60 °C, yellow block crystals can be acquired. Yield: 0.032 g, *ca.* 46.6%.

Preparation of HOF-TPPA

The suspension of TPPA-TMA soaked in phenethylamine (PEA) was centrifuged and washed with deionized water, and the solid powder obtained was dried. The dried solid powder was dissolved in ethanol (1 mL) and sonicated for 5 min, then deionized water (1 mL) was added and evaporated at room temperature for 5 days to obtain light yellow needle-like crystals.

Preparation of PEA-TMA

The suspension of TPPA-TMA after immersion in PEA was centrifuged and the complex of PEA and TMA was obtained by spinning the supernatant. This complex was dissolved in ethanol and sonicated for 5 min and volatilized at room temperature for 3 days to obtain colorless lumpy crystals.

Fabrication of TPPA-TMA Film

To uniformly disperse TPPA-TMA powder in agarose hydrogel (AG), the AG powder (70 mg) was added in 4 mL deionized water and the mixture was heated to 100 °C in an oil bath until AG powder was completely dissolved. Then TPPA-TMA powder (4 mg) was added in AG solution with continuous stirring. After mixed uniformly, the hot TPPA-TMA and AG mixed liquid was dropwise into the plastic mold with a diameter of 10 mm circular grooves and cooled for 10 min to form TPPA-TMA@AG Film.

Procedures for PEA detection

In a typical assay for PEA using the sensory material, 0.5 mg of TPPA-TMA ground powders were weighed and added to a 1.5 mL centrifuge tube containing the deionized water (1 mL) and a series of concentrations of fresh PEA aqueous solution (5×10^{-6}–10^{-3}M), followed by ultrasonication to form the uniform dispersion. Then, the prepared suspensions were transferred to fluorescence cuvettes with covers, and their luminescence spectra were measured in the 410–700 nm range under excitation at 360 nm. Test samples for the selectivity experiment were prepared with a similar procedure. Samples for specificity experiments were similarly prepared by adding TPPA-TMA into different chemicals mainly including (KCl, NaCl, lysozyme(Lys), NH_4Cl, $CaCl_2$, mucin, $MgCl_2$, α-amylase(Amy), Na_2CO_3, NaH_2PO_4, creatinine(Crea), creatine(Cre), glucose(Glu), uric acid(UA) and Na_2SO_4 10^{-3} M) in saliva and urine. These mixtures were then sonicated for luminescence measurements.

Saliva and urine sample preparation

The artificial saliva and urine samples were prepared using the reported procedures.[3]

Table S1. Crystal data and refinement parameters for **TPPA-TMA** and **HOF-TPPA**.

Identification code	TPPA-TMA	HOF-TPPA
Chemical formula	$C_{42}H_{30}N_4O_6$	$C_{33}H_{28}N_4O_2$
Formula weight	686.70	512.59
Crystal Colour	Yellow	Yellow
Temperature (K)	150	121
Crystal System	Triclinic	Monoclinic
Space Group	P-1	$P21/c$
a(Å)	11.6130(6)	10.0367(4)
b(Å)	13.3303(7)	23.407(1)
c(Å)	15.7331(7)	12.1733(5)
α(°)	93.278	90.000
β(°)	102.022	113.958
γ(°)	106.557	90.000
Z	2	4
V(Å³)	2265.7(2)	2613.5(2)
D_{calc}(g cm⁻³)	1.007	1.307
F(000)	716	716
R(int)	0.0855	0.062
Number of parameters	767	358
GOF on F^2	1.049	1.048
$R1^a$[I >2δ(I)]	0.0820	0.0408
wR_2^b(all data)	0.1829	0.097
CCDC	2205392	2256002

$R_1 = \Sigma(||Fo| - |Fc||)/\Sigma|Fo|$; $wR_2 = \{\Sigma w(|Fo|^2 - |Fc|^2)^2/\Sigma w(|Fo|^2)^2\}^{1/2}$.

Table S2 Crystal data and refinement parameters for **PEA-TMA**.

Identification code	PEA-TMA
Chemical formula	$C_{100}H_{122}O_{29}N_8$
Formula weight	1900.05
Crystal Colour	Colorless
Temperature (K)	150
Crystal System	Triclinic
Space Group	P-1
a(Å)	13.8836(5)
b(Å)	16.9212(5)
c(Å)	21.5095(7)
α(°)	90.265
β(°)	105.26
γ(°)	90.1
Z	2
V(Å^3)	4874.92(3)
D_{calc}(g cm^{-3})	1.294
F(000)	2020
R(int)	0.1041
Number of parameters	1367
GOF on F^2	1.029
$R1^a$[I >2δ(I)]	0.0732
wR_2^b(all data)	0.1957

$R_1 = \Sigma(||Fo| - |Fc||)/\Sigma|Fo|$; $wR_2 = \{\Sigma w(|Fo|^2 - |Fc|^2)^2/\Sigma w(|Fo|^2)^2\}^{1/2}$.
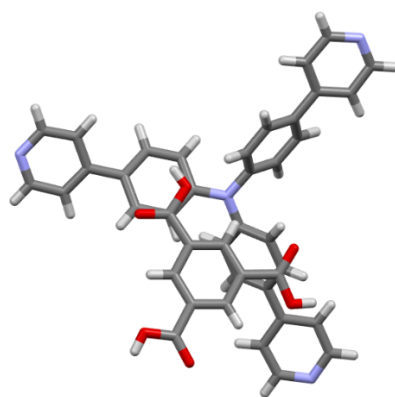
Fig. S1 The asymmetric unit of TPPA-TMA, C = grey, O = red, N = blue and H = white.
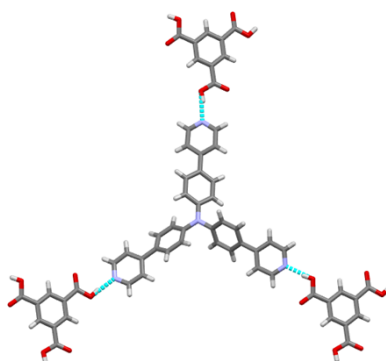
Fig. S2 The existence of three H_3TMA molecules around a TPPA molecule, forming O−H···N (cyan) hydrogen bonds.
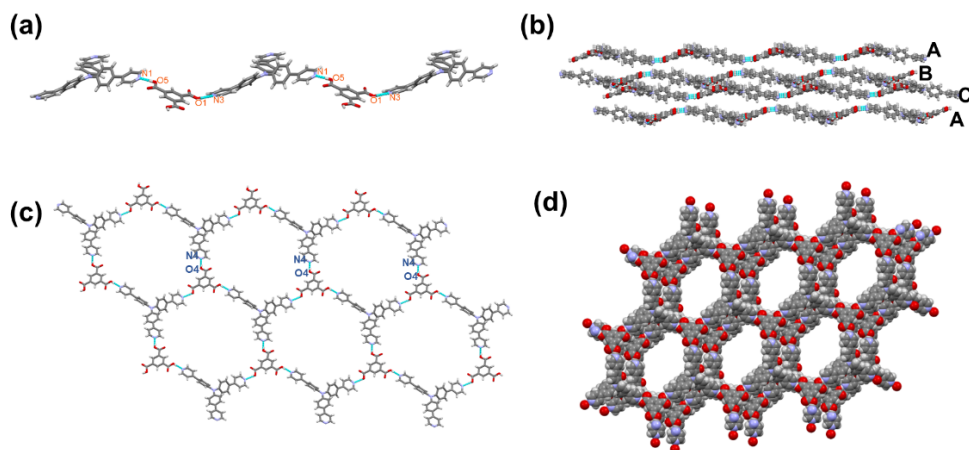
Fig. S3 The structural details of TPPA-TMA. (a) Adjacent TPPA and H_3TMA molecules linked by O5−H···N1 and O1−H···N3 bonds form a one-dimensional (1-D) chain. (b) and (d) The layers align in …ABCABC…sequence along the a-axis. (c) Adjacent 1-D chain connect with each other to form a 2-D layer based on hydrogen bond interaction (O4−H···N4).
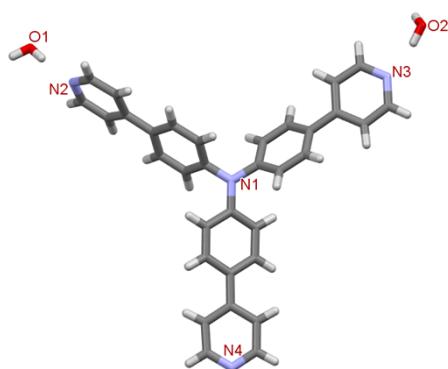
Fig. S4 The asymmetric unit of HOF-TPPA, C = grey, O = red, N = blue and H = white.
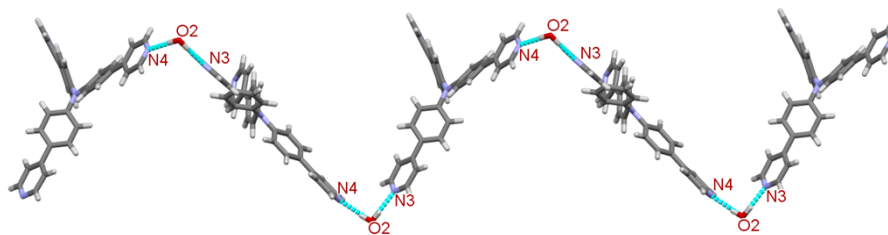
Fig. S5 Adjacent TPPA and H_2O molecules linked by O2–H···N4 and O2–H···N3 bonds form a one-dimensional (1-D) chain.
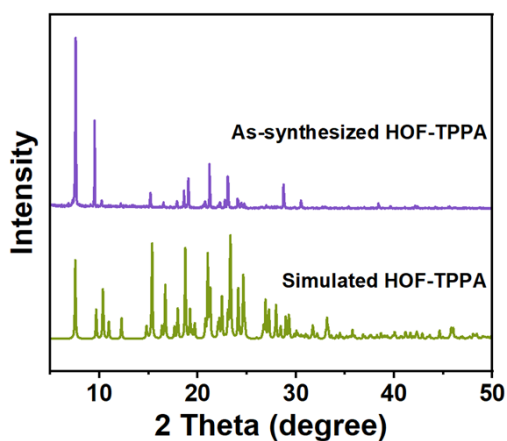
Fig. S6 PXRD patterns of simulated HOF-TPPA (green) and synthesised HOF-TPPA before (purple).
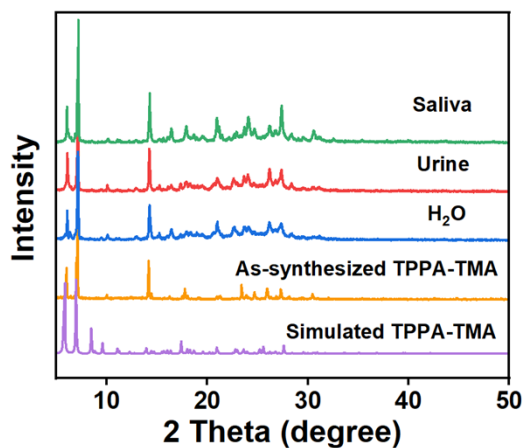
Fig. S7 PXRD patterns of TPPA-TMA after immersion in H_2O (blue), urine (red) and saliva (green).
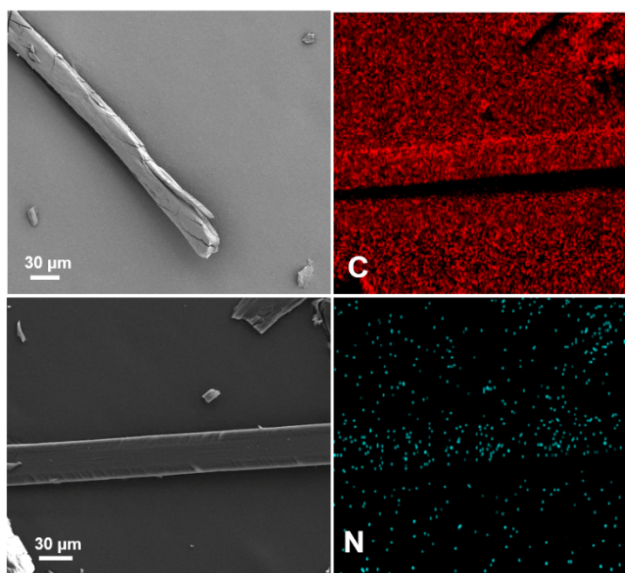
Fig. S8 SEM and elemental mapping images of HOF-TPPA.
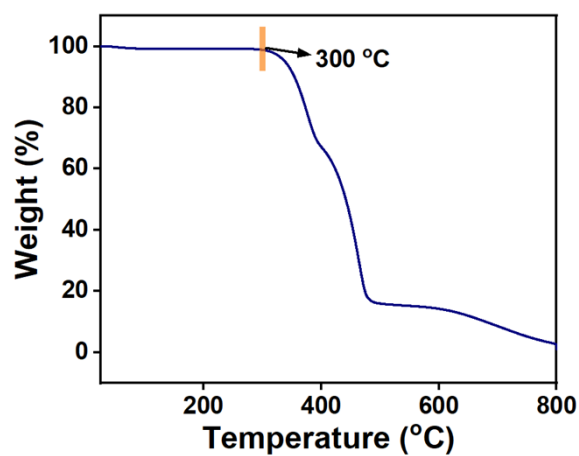
Fig. S9 TGA traces of TPPA-TMA ranging from room temperature to 800 °C.
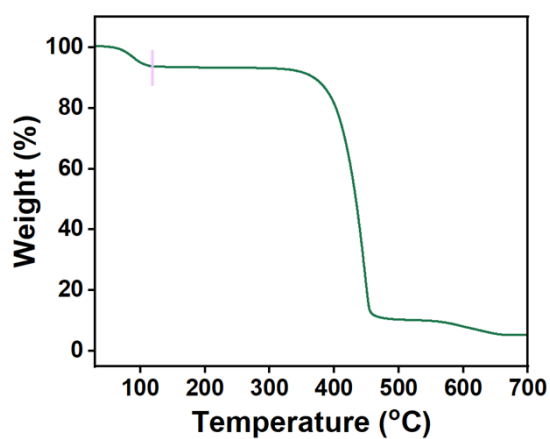
Fig. S10 TGA traces of HOF-TPPA ranging from room temperature to 700 °C.
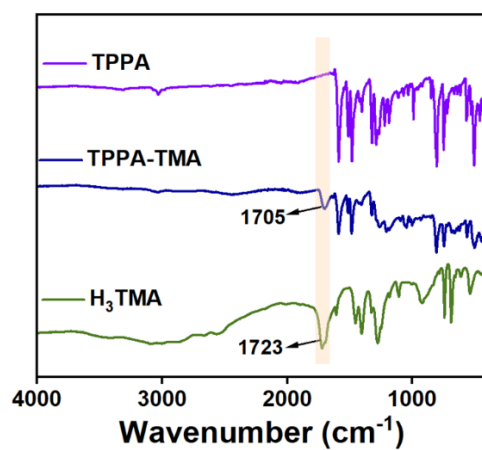
Fig. S11 FT-IR spectra of H_3TMA (green), TPPA-TMA (blue) and TPPA (purple).
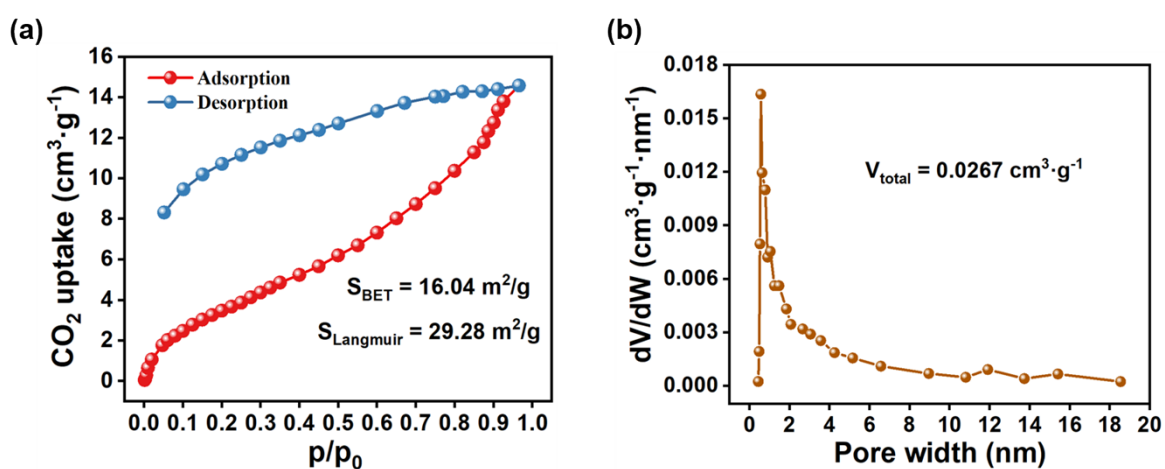
Fig. S12 (a) CO_2 adsorption-desorption isotherm of TPPA-TMA; (b) Pore size distribution of TPPA-TMA.
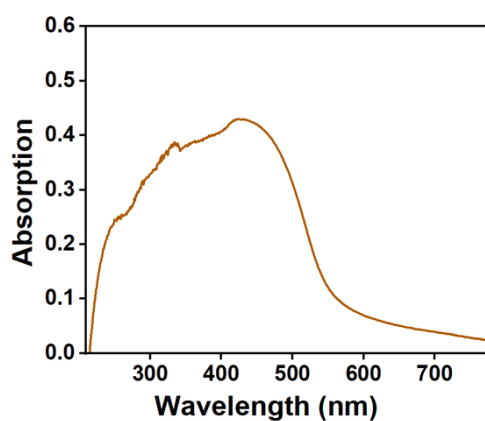
Fig. S13 The UV-vis absorption spectra for solid TPPA-TMA.
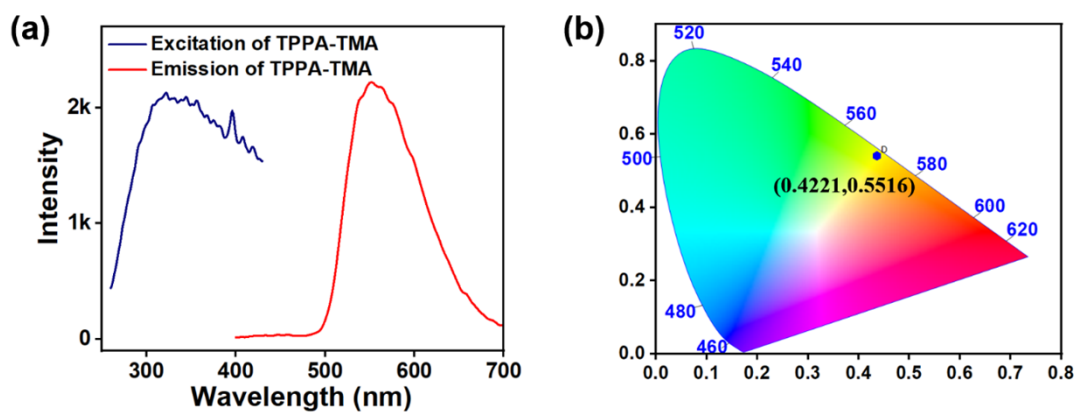
Fig. S14 (a) The excitation spectrum (λ_{em} = 550 nm) and emission spectra (λ_{ex} = 360 nm) of TPPA-TMA in aqueous solution. (b) The CIE chromaticity coordinates of TPPA-TMA in aqueous solution.
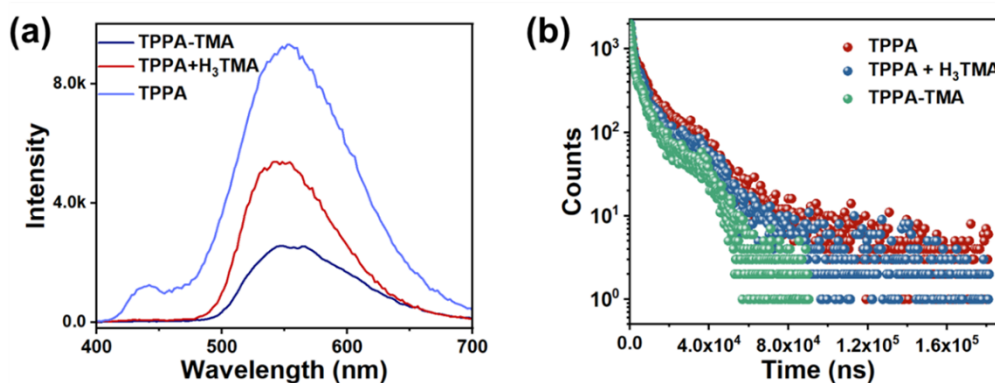
Fig. S15 (a) The emission spectras of TPPA (blue), TPPA+H$_3$TMA (red) and TPPA-TMA (navy green) in aqueous solution (λ_{ex} = 360 nm). (b) Decay lifetimes of 550 nm emission peak for TPPA (red), TPPA+H$_3$TMA (blue) and TPPA-TMA (green) (λ_{ex} = 360 nm).
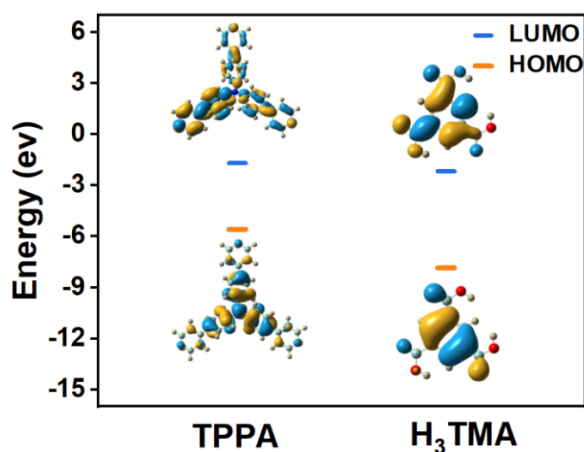
Fig. S16 The LUMO and HOMO orbitals of TPPA and H$_3$TMA.
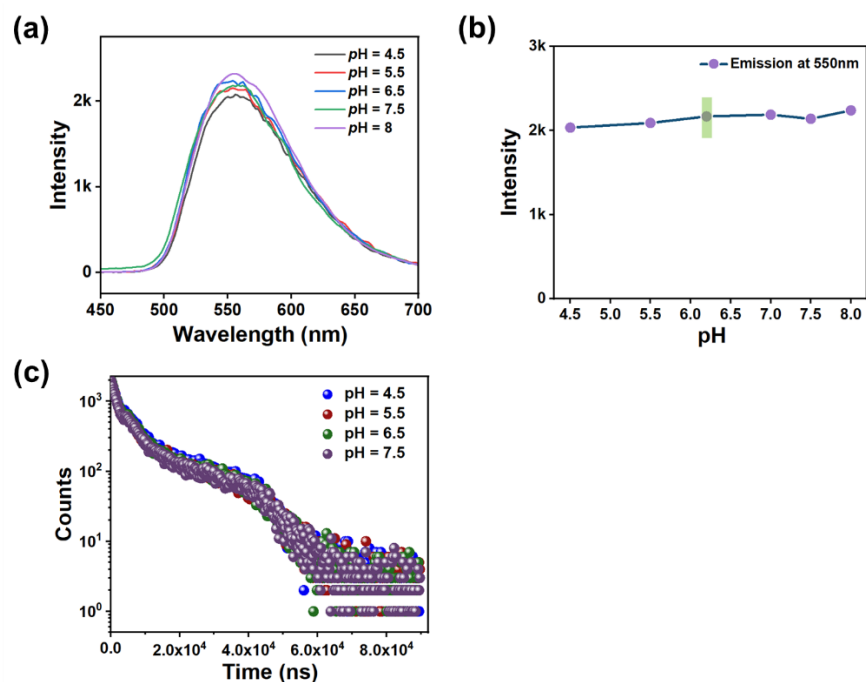
Fig. S17 Effects of *p*H on the emission spectrum (a) and luminescence intensities (b) of TPPA-TMA at 550 nm. The points marked with green bar represent the intensities of TPPA-TMA in deionized water (*p*H= 6.2). (c) Effects of *p*H on the decay lifetimes of TPPA-TMA at 550 nm.
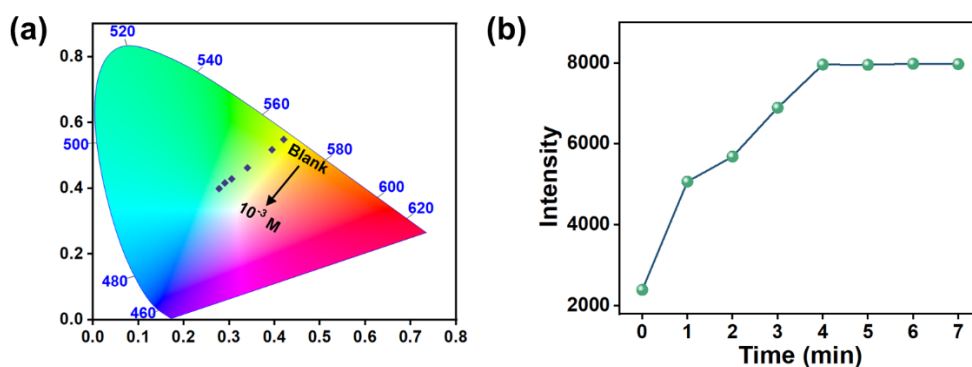
Fig. S18 (a) CIE chromaticity coordinates of TPPA-TMA in the presence of PEA at different concentrations under the excitation of 360 nm. (b) Time-response emission spectra of TPPA-TMA with 10^{-3} M PEA at 520 nm.
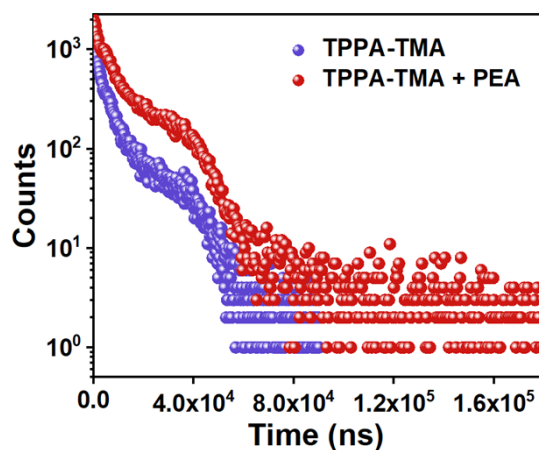

Fig. S19 Decay lifetimes of 550 nm emission peak for TPPA-TMA and TPPA-TMA+H_3TMA (C = 10^{-3} M) (λ_{ex} = 360 nm).

Table S3. Comparison of our sensor with other PEA sensors (limit of detection: LOD).

Analytical method	Linear range	LOD	Reference
Vacuum ultraviolet	6.25 – 200 µg mL^{-1}	2.13 µg mL^{-1}	1
Liquid Chromatography	0.50 – 30.0 µg L^{-1}	1.00 µg L^{-1}	2
Fluorescence	5–50 µM	1.05 µM	3
Electrochemical	10^{-8} – 8.0×10^{-5} M	8 nM	48
Electrochemical	10^{-7} – 10^{-2} M	1 µM	4
Electrochemical	3.0×10^{-5} – 6.1×10^{-4} M	1.3 µg mL^{-1}	5
Fluorescence	5×10^{-6} – 10^{-3} M	2.56 µM	This work
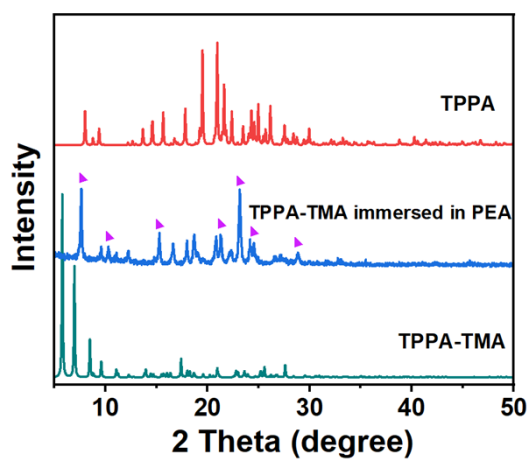
Fig. S20 PXRD patterns of TPPA-TMA, TPPA and TPPA-TMA treated with PEA (10^{-3} M). The purple triangles show the new generating peaks.
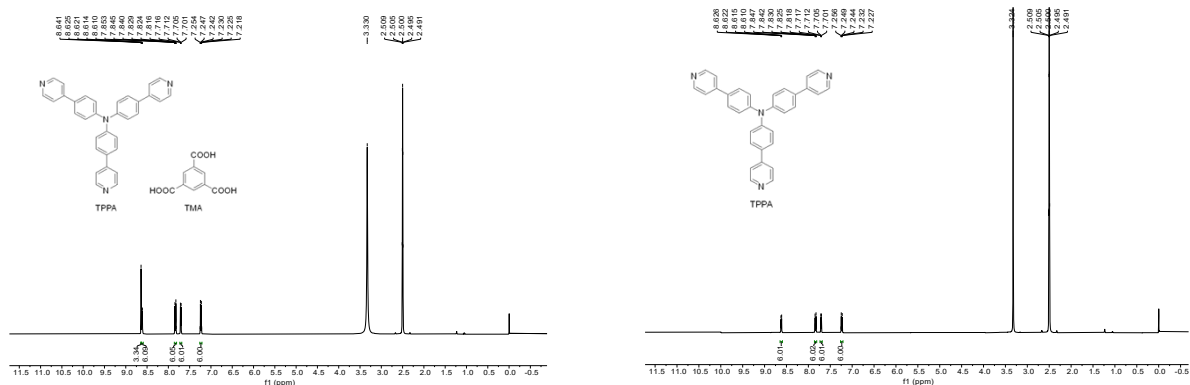
Fig. S21 ^{1}H NMR spectra of TPPA-TMA (a) and (b)TPPA-TMA treated with PEA (10^{-3} M).
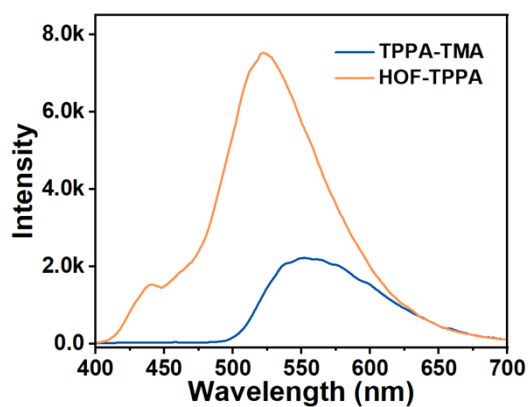
Fig. S22 The emission spectras of TPPA-TMA (blue) and HOF-TPPA (yellow) in aqueous solution (λ_{ex} = 360 nm).

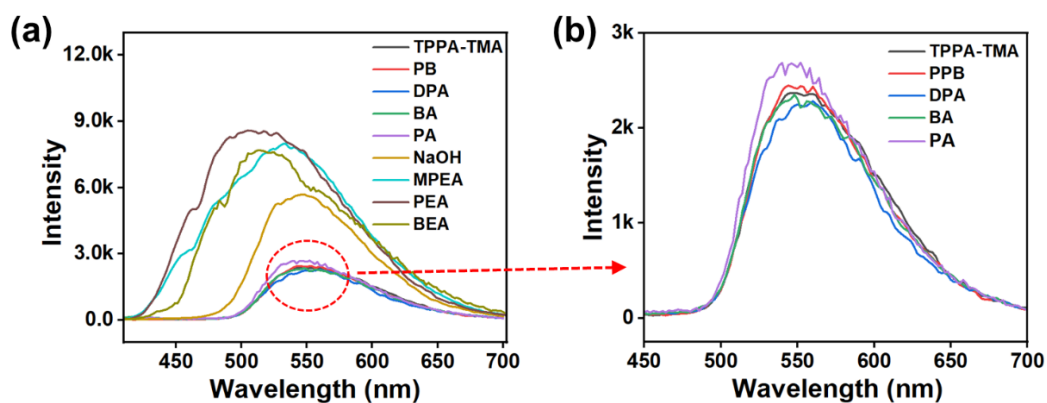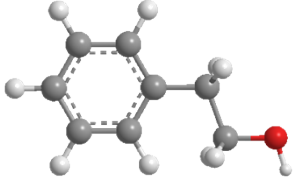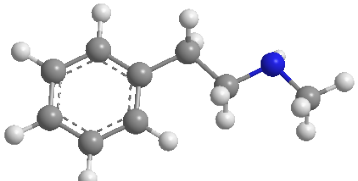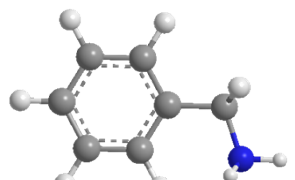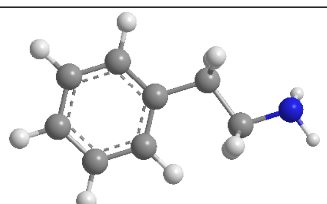**Fig. S23** (a) Fluorescence responses of TPPA-TMA to various aromatic analytes and NaOH (λ_{ex} = 360 nm). (b) Enlarged view of the red circle (fluorescence responses of TPPA-TMA to PPB, DPA, BA and PA).

Table S4. The structure and pH of aromatic analytes.

Entry	Substrate	Structure	pH
1	*n*-Propylbenzene (PPB)		5.65
2	Dopamine (DPA)		5.48
3	Benzenacetaldehyde (BA)		5.02

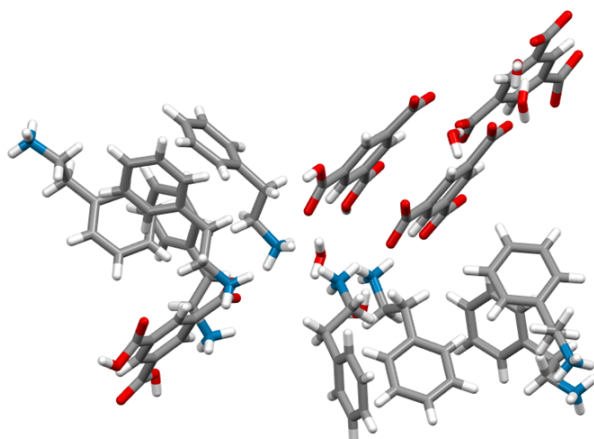|			
4	Phenethyl alcohol (PA)		5.68
5	*N*-methylphenethylamine (MPEA)		10.32
6	Benzylamine (BEA)		10.25
7	Phenylethylamine (PEA)		10.2

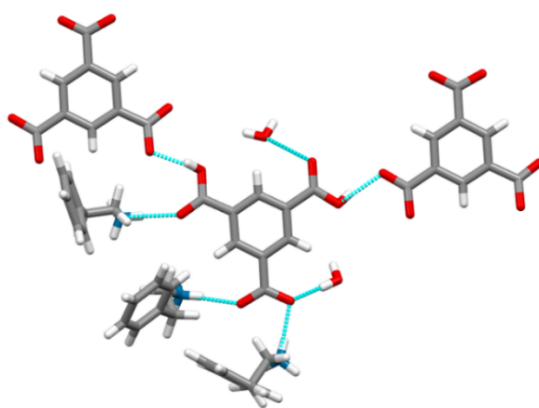**Fig. S24** The asymmetric unit of PEA-TMA, C = grey, O = red, N = blue and H = white.

Fig. S25 The existence of two TMA^{3-} anions, three PEAH^{+} cations and two H2O molecules around a H$_2$TMA^{-} anion, forming O−H···O and N−H···O hydrogen bonds.

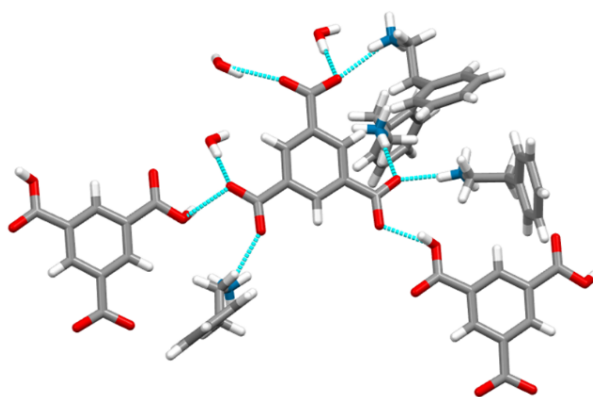**Fig. S26** The existence of two H$_2$TMA$^-$ anions, four PEAH$^+$ cations and three H2O molecules around a TMA^{3-} anion, forming O−H···O and N−H···O hydrogen bonds.
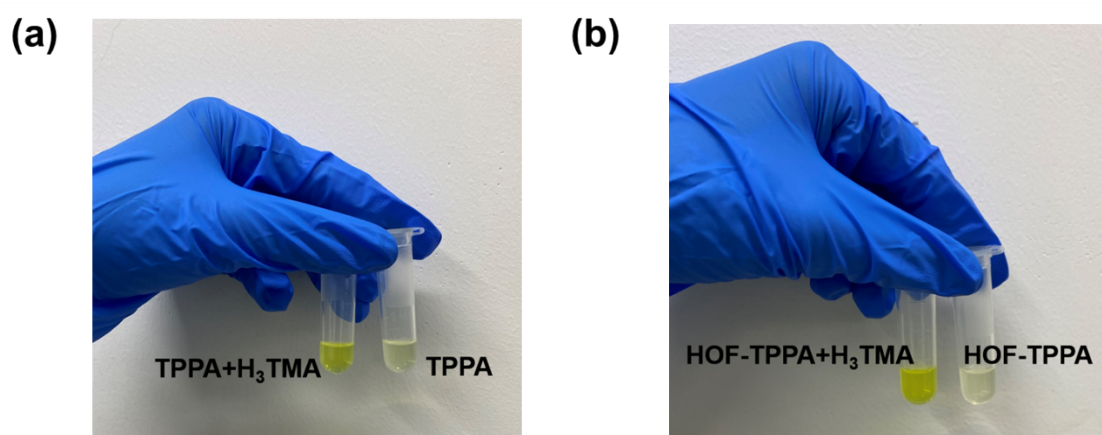

Fig. S27 (a) The colour change of TPPA solution before and after the addition of H$_3$TMA. (b) The colour change of HOF-TPPA solution before and after the addition of H$_3$TMA.
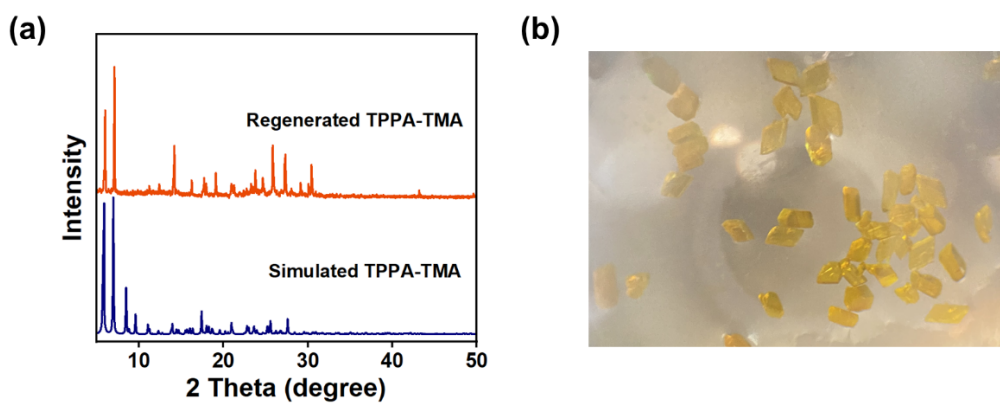

Fig. S28 (a) PXRD patterns of simulated TPPA-TMA (blue) and regenerated TPPA-TMA (red). (b) The picture of regenerated TPPA-TMA under the microscope.
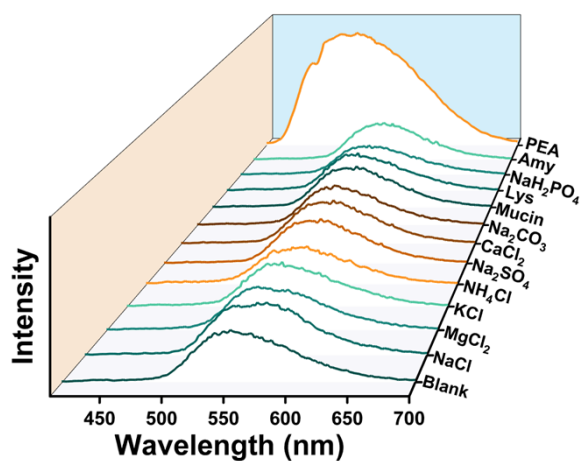
Fig. S29 The emission spectra of TPPA-TMA in PEA and various components (10^{-3} M) in saliva system.
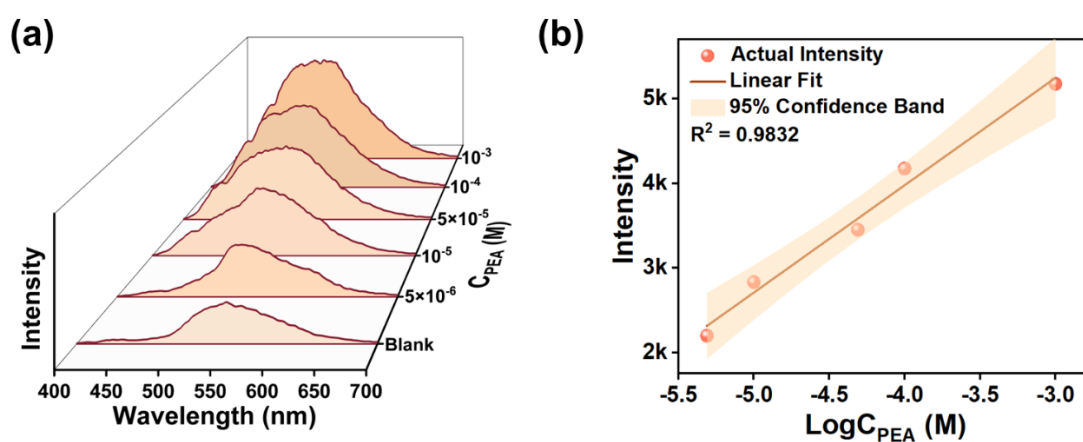

Fig. S30 (a) The emission spectrums (λ_{ex} = 360 nm) of TPPA-TMA immersed in various concentration of PEA in saliva (5×10^{-6} – 10^{-3} M). (b) Dependence of the emission intensity of TPPA-TMA on concentration of PEA in saliva.
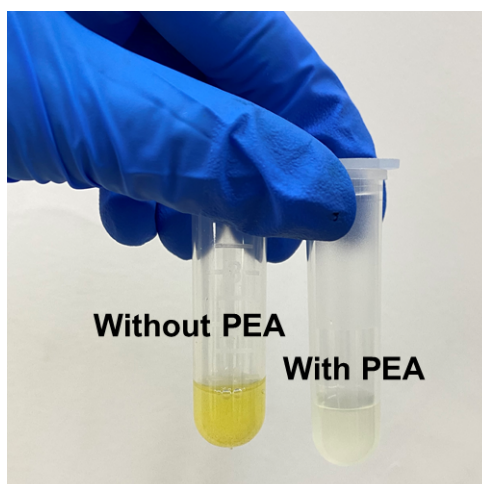

Fig. S31 The colour change of TPPA-TMA solution before and after the addition of PEA by the naked eye.
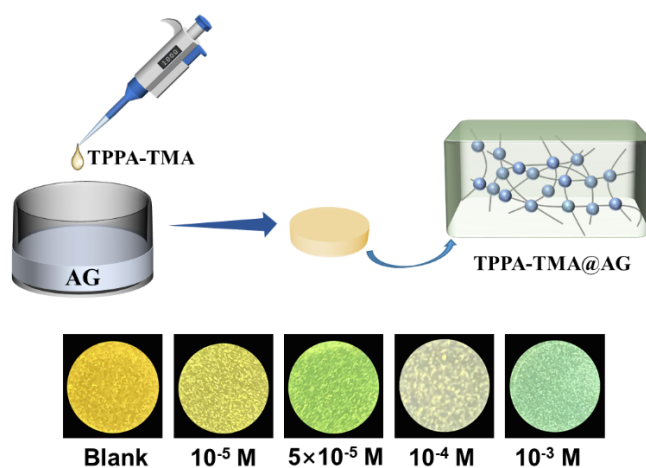
Fig. S32 The fabrication of TPPA-TMA@AG film and photographs of TPPA-TMA@AG soaked in various concentrations of PEA under 360 nm UV lamp.

Reference

[1] G. W. T. M. J. Frisch, H. B. Schlegel, G. E. Scuseria, M. A. Robb, J. R. Cheeseman, G. Scalmani, V. Barone, G. A. Petersson, H. Nakatsuji, X. Li, M. Caricato, A. Marenich, J. Bloino, B. G. Janesko, R. Gomperts, B. Mennucci, H. P. Hratchian, J. V. Ortiz, A. F. Izmaylov, J. L. Sonnenberg, D. Williams-Young, F. Ding, F. Lipparini, F. Egidi, J. Goings, B. Peng, A. Petrone, T. Henderson, D. Ranasinghe, V. G. Zakrzewski, J. Gao, N. Rega, G. Zheng, W. Liang, M. Hada, M. Ehara, K. Toyota, R. Fukuda, J. Hasegawa, M. Ishida, T. Nakajima, Y. Honda, O. Kitao, H. Nakai, T. Vreven, K. Throssell, J. A. Montgomery, Jr., J. E. Peralta, F. Ogliaro, M. Bearpark, J. J. Heyd, E. Brothers, K. N. Kudin, V. N. Staroverov, T. Keith, R. Kobayashi, J. Normand, K. Raghavachari, A. Rendell, J. C. Burant, S. S. Iyengar, J. Tomasi, M. Cossi, J. M. Millam, M. Klene, C. Adamo, R. Cammi, J. W. Ochterski, R. L. Martin, K. Morokuma, O. Farkas, J. B. Foresman, and D. J. Fox, Gaussian 09, Revision D.01; Gaussian, Inc.: Wallingford CT, 2013.

[2] S. Grimme, J. Antony, S. Ehrlich, H. Krieg, *J. Chem. Phys.* **2010**, *132*, 154104.

[3] Z. Hu, B. Yan, *J. Mater. Chem. A* **2023**, *11*, 4739-4750.